

In vivo quantitative lipidic map of brown adipose tissue by chemical shift imaging at 4.7 tesla

Ernesto Lunati,^{*,†} Pasquina Marzola,^{*} Elena Nicolato,^{*} Mauro Fedrigo,[§] Marco Villa,[†] and Andrea Sbarbati^{1,*}

Magnetic Resonance Laboratory,^{*} Institute of Human Anatomy and Histology, University of Verona, Verona, Italy; INFM Unit,[†] University of Pavia, Italy; and Bruker Spectrospin Italia,[§] Milano, Italy

Abstract In the present paper, chemical shift imaging techniques are applied to quantitative in vivo evaluation of fat and water content in interscapular brown adipose tissue (BAT). The experiments have been carried out on five female Sprague-Dawley rats after calibration and testing with suitable phantoms containing known amounts of water and oil. We found that, in the interscapular BAT, the fat is about 50% at the surface (mainly unilocular) region, but its percentage drops to 20–30% in the deepest (mainly multilocular) portion. The perirenal deposits of white adipose tissue (WAT) contained significantly higher amount of fat with large areas ranging from 70 to 90%. Later the rats were killed and the same procedure was repeated with dead animals. Experiments performed in dead rats show a modification of the hydro-lipidic ratio more evident in the multilocular portions of the deposit. **■** The present work demonstrates that MRI-based methods allow a non-invasive, in vivo quantitative mapping of the lipid content which can be applied to investigation of brown adipose tissue deposits in small experiment animals.—Lunati, E., P. Marzola, E. Nicolato, M. Fedrigo, M. Villa, and A. Sbarbati. **In vivo quantitative lipidic map of brown adipose tissue by chemical shift imaging at 4.7 tesla.** *J. Lipid Res.* 1999. 40: 1395–1400.

Supplementary key words NMR • adipocytes • fat

The lipid content of brown fat cells roughly mirrors their functional status, being high in the nearly quiescent cells and low in the thermogenically active cells (1). Magnetic resonance imaging (MRI) is a technique which allows discriminating brown adipose tissue (BAT) deposits from the more abundant white adipose tissue (WAT) deposits (2). Therefore MRI seems to be appropriate for an in vivo morphological investigation of small deposits of BAT. Furthermore, the MRI data yield information about histology (3), functional state (4), or pathology of a localized region of the tissue (5). In a previous study (6) we have shown that chemical shift imaging (CSI) techniques (7) may be used to identify BAT and to discriminate it from other tissues. The purpose of this work is to show that CSI also leads to a reliable and quantitative evaluation of fat and water content of BAT tissue.

Several techniques have been proposed in biomedical MRI to obtain separate images of water and fat protons in tissues and to evaluate the ratio between these components (7). At low magnetic field, the Dixon method (8), based upon the dephasing of fat and water signal, may be applied, and included also in fast gradient-echo sequences (9). At high magnetic fields, where the Dixon method is limited by susceptibility effects (7), the chemical shift between water and fat proton ($-OH$, $-CH_2$) yields frequency separations large enough to permit selective excitations of fat or water proton. In this way, a “water image” and a “fat image” may be obtained. Excellent field homogeneity, achieved by shimming over the sensitive volume of the coil, is needed to reduce the widths of these signals.

In this work we apply a spin-echo (SE) sequence with selective excitation to acquire fat and water images of the interscapular brown adipose tissue (IBAT) in living rats. After applying corrections for relaxation effects (10), the images yield quantitative maps of fat and water contents with submillimetric resolution. The aim of this work is to propose a new method, which would yield quantitative maps of fat fractions in BAT, suitable to follow, in vivo and over time, the functional status of BAT. As such, we can say that this method could represent a kind of functional imaging for studying adipose tissues.

MATERIALS AND METHODS

Experimental

All experiments were carried out using an SIS 200/330 imager spectrometer (SIS Co., Fremont, CA) equipped with a 4.7 T Oxford magnet and SMIS (Surrey Medical Imaging Systems Ltd, UK) gradient insert. A 5 cm i.d. home-made saddle coil was used.

We acquired two series of chemical shift selective images, one

Abbreviations: BAT, brown adipose tissue; IBAT, interscapular brown adipose tissue; WAT, white adipose tissue; CSI, chemical shift imaging; MRI, magnetic resonance imaging; SE, spin-echo; ppm, parts per million.

¹ To whom correspondence should be addressed.

for fat protons and one for water protons. Each series consisted of a multiple-echo sequence, with TR = 1600 ms, TE = 15, 30, 45 ms and two single-echo sequences (TE = 15 ms) acquired with TR = 800, 400 ms. T2 maps were obtained by fitting the multiple echo images while T1 maps were obtained by fitting the images acquired with TR = 1600, 800, 400 ms and TE = 15 ms. In both the multi-echo and single echo sequence, the chemical shift selection is performed by the 180° refocusing pulse (7). Both the 90° and the 180° pulses are band-selective Gaussian pulses; however, the 90° is applied when the slice-selection gradient is on, while the 180° pulse is applied with all gradients off, to refocus only the selected chemical-shift range. The 180° pulse was a 4 ms Gaussian pulse which excites a 500 Hz bandwidth, appropriate to discriminate fat and water peaks which, at 4.7 T, have a separation of about 700 Hz. All images were acquired using the following parameters: FOV = 5 cm × 5 cm, matrix size 128 × 128, NEX = 2, slice thickness = 2 mm, pixel size = 0.4 mm.

The method was tested using phantoms of vegetable oil prepared according to Poon et al. (10). Briefly, the phantoms were made by mixing known amounts of water (doped with 0.2 mM MnCl₂) and vegetable oil (Peanut oil, Esselunga, Limoto, Italy) containing 2% of Tween 80 (poly-oxyethylene sorbitan monooleate, Sigma Aldrich) (10). The mixtures, homogeneously mixed by ultrasonic disruption, contained respectively 0%, 20%, 40%, 60%, and 80% of oil by volume. Fifteen-mm diameter plastic tubes, placed longitudinally into the magnet, were used and transverse images were acquired twice. The sonicated lipid mixture remained homogeneously dispersed throughout image acquisition.

A group of five female Sprague-Dawley rats, 6-weeks-old and weighing 150 g each, was anesthetized by inhalation of O₂ containing 1–2% halothane. The IBAT deposit was initially located with a scout image. A single transverse 2-mm thick slice was positioned in the middle of this tissue for CSI acquisitions. The acquisition time was about 20 min. Neither cardiac nor respiratory gating were used during acquisition as we found that these experiments did not suffer motion artifacts. The rats were subsequently killed with an overdose of pentobarbital, and the imaging procedure was repeated with the dead animals. Although with dead animals it was possible to acquire more images giving better T1 and T2 fits, we preferred to repeat exactly the same protocol in order to compare equivalent data. Image processing was performed with our own package for calculations of T1 and T2 maps, and with the Khoros package (11, 12) for the remaining procedures.

A further group of four rats, 6-weeks-old and weighing 150 g each, was killed with ether; the intermediate portion of the IBAT deposit was microdissected out free of contaminant white fat, and weighed fresh. The specimens were freeze-dried (Modulyo, Edwards) until their weight remained constant (about 48 h) and the gravimetric evaluations were repeated. The water contents was expressed as mean ± SD.

Calculation of lipid maps

The signal intensities of fat and water are a function of their respective proton densities, but depend also upon relaxation times and experimental parameters. For a spin-echo sequence, the signal intensity *S* may be written as

$$S = k\rho \exp\left(-\frac{TE}{T2}\right) \left[1 - 2 \exp\left(-\frac{TR - TE/2}{T1}\right) + \exp\left(-\frac{TR}{T1}\right) \right] \quad \text{Eq. 1}$$

where *k* is a scaling factor, ρ the proton density, *TR* and *TE* the repetition and echo times, *T1* and *T2* are the longitudinal and transverse relaxation times (10). Quantitation of the fat and water proton content requires the retrieval of ρ from *S* through estimation of the factors which depend upon experimental and re-

laxation times. Fat and water *T1* and *T2* were evaluated pixel by pixel using algorithms tailored to spin-echo images. Because transverse relaxation is essentially a single exponential process, *T2* was obtained through a least squares linear fitting of the logarithms of the pixel intensities versus *TE*. For the *T1* calculation, as spin-lattice relaxation may be usually described with a bi-exponential decay (see Eq. 1), a non-linear iterative fitting procedure, based upon the Levenberg-Marquadt algorithm (13) was used to retrieve *T1* values appropriate for the different experiments. Statistical methods are used to validate the *T1* and *T2* estimates.

After the maps of the relaxation times have been obtained, through a reconstruction based on the inverse of Eq. 1, the maps of water and fat proton densities, ρ_f and ρ_w , were produced. Finally, also the fraction of fat *f* was calculated pixel by pixel as

$$f = \frac{\rho_f}{\rho_f + \rho_w R} \quad \text{Eq. 2}$$

where *R* is the ratio of the fat to water proton densities in their pure form: a value *R* = 0.9 has been used as in literature (10). The water fraction by volume of the sample is obviously 1 - *f*. Some voxels in the boundary areas undergo partial-volume effects, but the small pixel size greatly reduces this problem and allows a correct average evaluation in the different portions of the tissue.

Values of mean lipid percentage have been calculated in region of interest and averaged over the animals. The results were calculated in the form "mean ± SEM" and statistical analysis was performed by a two-sided paired *t*-test.

RESULTS

Our method of quantitative evaluation of fat content has been tested in phantoms. In Fig. 1, we compare the "known values" of the fat contents, measured gravimetrically, of the phantoms, with the "experimental values" provided by our MRI method. The experimental values were

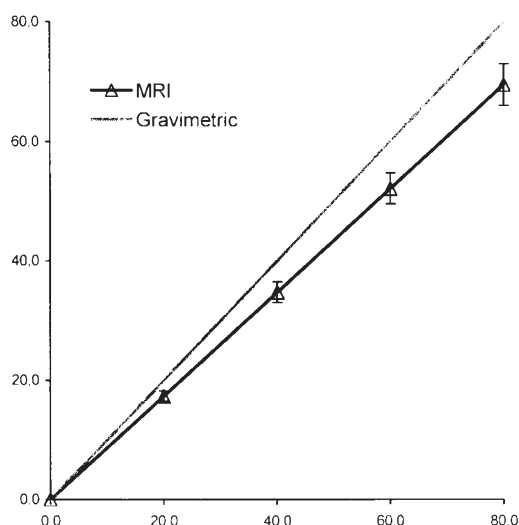


Fig. 1. Analysis of phantoms of vegetable oil prepared according to Poon et al. (10). Comparison between the percentage of oil by volume using volumetric measurement (real fat content) and MRI-measured fat contents. The MRI measures, repeated twice with error <5%, are fitted by a straight line passing through the origin with slope = 0.868, and present a high correlation with the gravimetric measures ($r^2 = 0.999$).

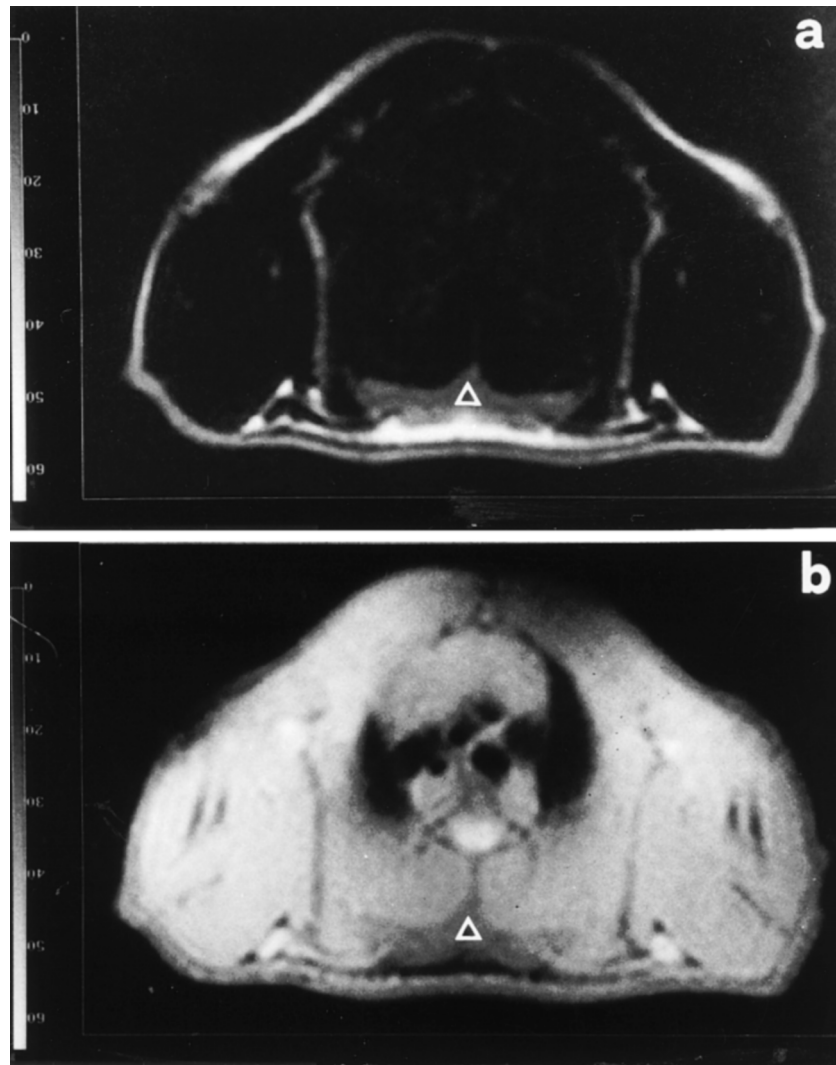


Fig. 2. Transverse section at the level of the interscapular BAT of a living rat. (a) Fat image; (b) water image. IBAT is marked by a triangle.

obtained by choosing a ROI (region-of-interest) enclosing nearly the full section of the tubes. Two repeated measurements provided the same results up to the second significant digit. The MRI data present a high correlation with the gravimetric ones ($r^2 = 0.999$), but the slope of the fitting straight line is 0.868 instead of 1 (gray line in Fig. 1), indicating that some kind of systematic underestimation exists. The fat fraction is underestimated by about 10%, so the agreement is still good at low fat contents, as is the case of IBAT.

In vivo evaluations of fat and water content were performed upon the IBAT, which is a well characterized model. **Figures 2a** and **b** show fat selective and water selective SE images acquired in the transverse plane on the IBAT deposit. It is apparent that the IBAT deposit is roughly “crown shaped” and consists of a central mass with lateral wings. **Figure 3**, top presents the map of the lipid fraction computed from the same data reported in Fig. 2; Fig. 3, bottom shows the IBAT region magnified. We may divide the interscapular deposit in three regions,

as shown in **Fig. 4**: two parallel, trapezoidal layers and a third layer that encloses the wings. Values of mean lipid percentage have been calculated in each region and averaged over the five animals. The results are reported in **Table 1**. The external layer contains about 50% of fat, while the intermediate layer and the wings contain about 30% and 20% of fat, respectively. The external layer is not clearly separated from the overlying subcutaneous WAT tissue, but we assumed the last to have roughly the same thickness here as elsewhere. A systematic observation of the different WAT deposits has not been done; however, for comparison with these results, we observed that the perirenal WAT contained significantly higher amount of fat with large areas ranging from 70 to 90% (these data were obtained from lipidic maps generated with the same method as the IBAT maps).

The fat content of the IBAT was evaluated on the same animals immediately after cardio-circulatory arrest. **Figure 5** shows the comparison between the lipid percentage map calculated for a living rat and the same map calcu-

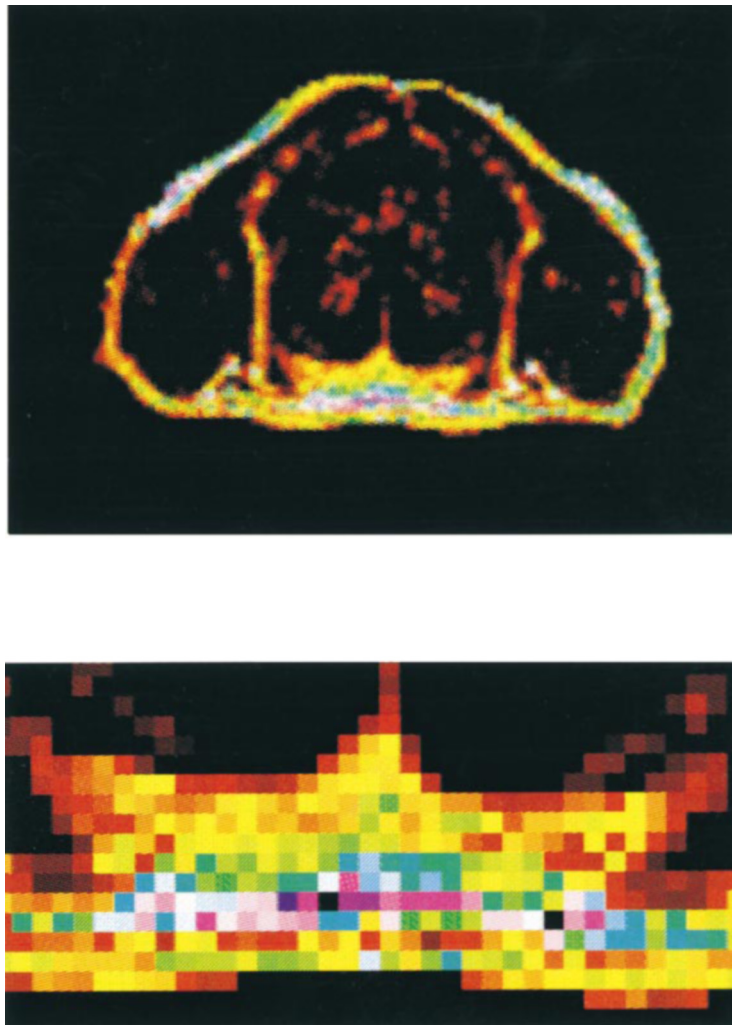


Fig. 3. Top: Color map of the lipid fraction in the transverse section of a living rat; the transverse section is the same as in Fig. 2. Bottom: Magnified interscapular BAT.

lated for a dead rat. The results, summarized in Table 1, show that an apparent increase in the lipid content occurs in dead rats. Such a modification is particularly pronounced (about 10%) in the intermediate IBAT layer.

In this latter portion of the IBAT, the gravimetric evaluations of the microdissected specimens revealed a

water content $57.7 \pm 2.8\%$ very close to the value calculated by MRI.

DISCUSSION

Our previous studies (4, 6) demonstrated that MRI can provide an *in vivo* characterization of adipose tissues and of BAT in particular. A qualitative analysis based upon CSI

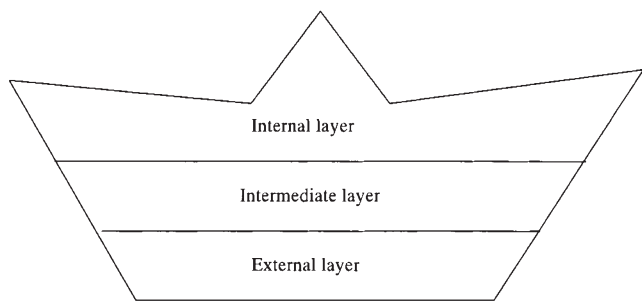


Fig. 4. Sketch of the layers of the interscapular BAT deposit, which identifies the regions reported in Table I. Values of mean lipid percentage have been calculated in each region and averaged over the rats.

TABLE 1. Fat content in rat IBAT

Tissue	Fat Content	
	Living	Dead
	%	
External layer ^a	52.5 ± 3.0	62.0 ± 2.2
Intermediate layer ^b	28.4 ± 8.0	41.6 ± 4.7
Internal layer	21.7 ± 7.7	25.9 ± 6.9

^a The difference between living and dead is significant according to the *t*-test with $P < 0.02$.

^b The difference is significant with $P < 0.05$.

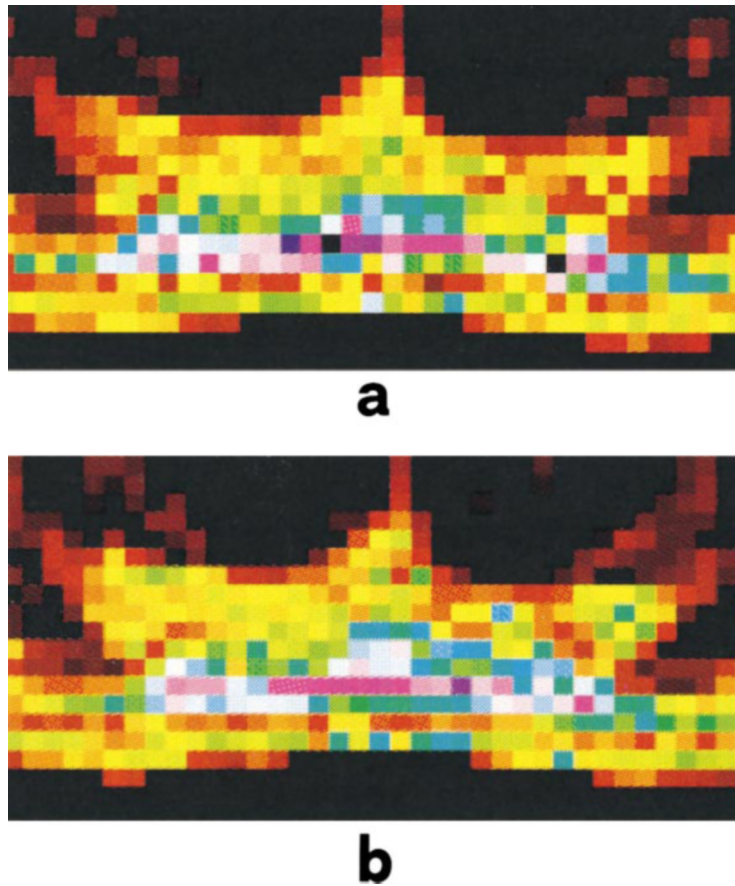



Fig. 5. Comparison between map of lipid fraction in living (a) and dead rat (b).

sequence was sufficient to discriminate BAT from other tissues. However, the characterization of BAT is substantially improved by a quantitative determination of fat and water fraction of the adipose deposits. This study demonstrates the feasibility of quantitating water content in the interscapular BAT of rats at 4.7 T. The accuracy of the quantification, as tested in phantoms and in microdissected specimens, was generally satisfactory but somehow reduced at the highest lipid concentration, as already noted by several authors (7, 14, 15).

Through our quantitative analysis of the fat content, we have obtained a novel and interesting representation of the interscapular deposit, which consists of three layers with different concentrations of fat. The surface layer, which is in contact with the subcutaneous WAT, is the most rich in lipids. The deepest portion of the IBAT, which extends toward the muscular tissue, is rich in water. Such a representation substantially agrees with observations from histology and ultrastructural examination (16). Furthermore, our data are consistent with biochemical evaluations of the triglyceride content (1). Compared with biochemical evaluations, our method accurately shows the spatial distribution of the lipid and may be repeatedly applied to the same animal, to follow evolution of fat tissues under different experimental conditions, as MRI is inherently non-invasive.

Our study demonstrates that the multilocular portion

(3) of the IBAT contains less than 30% of fat while the unilocular component has lipid fraction close to 50%. It must be stressed that this component histologically resembles the WAT, although the latter has a fat percentage that reaches peak values of 80% or higher (6). The differences observed in the fat content of IBAT between living and dead animals requires further discussion. At present, we do not have a certain physiological explanation of the phenomenon. The increase is apparently more pronounced in the multilocular portion of the deposit relative to the unilocular one. Because the multilocular portion is more vascularized than the unilocular one, circulatory effects may play a role. In any case, the phenomenon is evidence of the fact that functional parameters of the tissue influence the image obtained *in vivo*.

In this study we have demonstrated that our method can produce quantitative maps of fat fractions in BAT and for this reason is suitable to follow the functional status of BAT over time, allowing a kind of functional imaging for studying adipose tissues. 

This work was supported by grants from the Italian Ministry of University and Scientific Research (MURST), the Italian National Research Council (CNR), and the European Union (EU).

Manuscript received 10 August 1998 and in revised form 30 December 1998, and in re-revised form 19 February 1999.

REFERENCES

1. Senault, C., G. Cherqui, M. Cadot, and R. Portet. 1981. Cold-induced developmental changes in fat cell size and number in brown adipose tissue of the rat. *Am. J. Physiol.* **240**: E379–E388.
2. Osculati, F., F. Leclercq, A. Sbarbati, C. Zancanaro, S. Cinti, and K. Antonakis. 1989. Morphological identification of brown adipose tissue by magnetic resonance imaging in the rat. *Eur. J. Radiol.* **9**: 112–114.
3. Sbarbati, A., M. Morroni, C. Zancanaro, and S. Cinti, 1991. Rat interscapular brown adipose tissue at different ages: a morphometric study. *Int. J. Obes.* **15**: 581–588.
4. Sbarbati, A., A. M. Baldassarri, C. Zancanaro, A. Boicelli, and F. Osculati. 1991. In vivo morphometry and functional morphology of brown adipose tissue by magnetic resonance imaging. *Anat. Rec.* **231**: 293–297.
5. Sbarbati, A., F. Leclercq, F. Osculati, and I. Gresser. 1995. Interferon α/β -induced abnormalities in adipocytes of suckling mice. *Biol. Cell.* **83**: 163–167.
6. Sbarbati, A., U. Guerrini, P. Marzola, R. Asperio, and F. Osculati. 1997. Chemical shift imaging at 4.7 tesla of brown adipose tissue. *J. Lipid Res.* **38**: 343–347.
7. Kaldoudi, E., and S. C. R. Williams. 1992. Fat and water differentiation by Nuclear Magnetic Resonance Imaging. *Concepts Magn. Reson.* **4**: 53–71.
8. Dixon, W. T. 1984. Simple proton spectroscopic imaging. *Radiology.* **153**: 189–194.
9. Fishbein, M. H., K. G. Gardner, C. J. Potter, P. Schmalbrock, and M. A. Smith. 1997. Introduction of fast MR imaging in the assessment of hepatic steatosis. *Magn. Reson. Imaging.* **15**: 287–293.
10. Poon C. S., J. Szumowski, D. B. Plewes, P. Ashby, and R. M. Henkelman. 1989. Fat/water quantitation and differential relaxation time measurement using chemical shift imaging technique. *Magn. Reson. Imaging.* **7**: 369–382.
11. P. Marzola, A. Da Pra, A. Sbarbati, and F. Osculati. 1998. A PC-based workstation or processing and analysis of MRI data. *Magma.* **7**: 16–20.
12. Khoral Research Inc., Albuquerque, NM. Khoros Software. <http://www.khoral.com/>
13. Press, W. H., B. P. Flannery, S. A. Teukolsky, and W. T. Vetterling. 1988. Numerical Recipes in C: the Art of Scientific Computing. Cambridge University Press, Cambridge.
14. Brix, G., S. Heiland, M. E. Bellemann, T. Koch, and W. J. Lorenz. 1993. MR Imaging of fat-containing tissues: valuation of two quantitative imaging techniques in comparison with localized proton spectroscopy. *Magn. Reson. Imaging.* **11**: 977–991.
15. Graham, S. J., and M. J. Bronskill. 1996. MR measurement of relative water content and multicomponent T_2 relaxation in human breast. *Magn. Reson. Med.* **35**: 706–715.
16. Osculati, F., A. Sbarbati, F. Leclercq, C. Zancanaro, C. Accordini, K. Antonakis, A. Boicelli, and S. Cinti. 1991. The correlation between magnetic resonance imaging and ultrastructural patterns of brown adipose tissue. *J. Submicrosc. Cytol. Pathol.* **23**: 167–174.